Control Relevant Identification and Servo Design for a Compact Disc Player

Paul M.J. Van den Hof[1] and Raymond A. de Callafon[2]

[1] Signals, Systems and Control Group, Department of Applied Physics, Delft University of Technology, 2628 CJ Delft, The Netherlands
[2] Department of Mechanical and Aerospace Engineering, University of California at San Diego, 9500 Gilman Drive, La Jolla, CA 92093-0411, USA.

Abstract. The application of control relevant modeling of a radial servo loop in a CD (Compact Disc) player is presented in this chapter. The modeling is based on an identification algorithm that uses experimental data obtained from closed-loop experiments to find a low-order feedback relevant linear discrete time model for model-based servo control design. In this procedure a plant model is identified in terms of a normalized coprime factorization. Enhanced performance controllers are designed and implemented, and it is shown how estimated model uncertainty bounds can be used to verify robust stability of the designed controller prior to implementation.

1 Introduction

The control relevant identification approach discussed in this chapter illustrates the development of a dynamical model of a CD (Compact Disc) radial positioning mechanism. The intention of this application is to focus on the closed-loop approximate identification of the radial actuator in a CD player and on improved servo track following properties by designing a high-performance servo controller.

An increasing amount of rotational data storage applications such as Hard Disc Drives or CD players are used in portable applications subjected to shock disturbances. The shock resistance of such a storage device operating can be improved by designing a high-performance track following servo controller. As a result, the application of a control relevant identification algorithm to the radial servo loop in the CD player discussed in the application of this chapter is faced with several interesting challenges:

- the radial actuator exhibits a marginally stable open loop behavior and has multiple lightly damped mechanical resonance modes;
- due to the operating conditions of the CD player, the identification procedure is required to estimate models on the basis of closed-loop experiments only;
- finally, the models of the CD radial actuator are required to be suitable for servo control design.

The first two items illustrate the nature of the system to be modelled and controlled. More details on the radial mechanism in the CD player are given in Section 2. The latter item illustrates that models used for control design are necessarily approximative. On the one hand exact modeling can be impossible or too costly, on the other hand control design methods can get unmanageable if they are applied to models of high complexity. For example, a highly complex (and high-order) finite element model is useful for mechanical design considerations. However, for servo design purposes a low-order (approximate) model is needed for a manageable feedback control design.

In the application of the CD radial servo mechanism discussed in this chapter, the above mentioned challenges are tackled by adopting a control-relevant identification framework based on fractional model representations. In line with the idea of iterative identification and control [5,10] the aim is to identify a limited-order approximate model to be used as a basis for enhanced control design, on the basis of experiments performed under closed-loop conditions. More details on this framework are given in Section 6. First, a description of the CD radial servo loop is given in the following section.

2 The Compact Disc Mechanism

The CD mechanism considered in this application is a Philips CDM9 mechanism. The CDM9 consists of a turn table DC-motor for the rotation of the Compact Disc and a radial actuator with an Optical Pick-up Unit (OPU) that emits a laser spot for data reading. A schematic impression of the CD

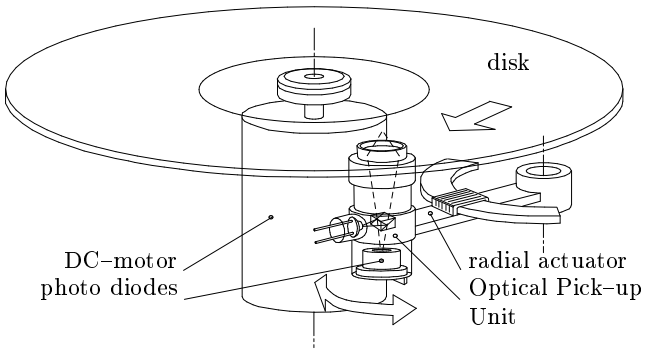

Fig. 1. Schematic view of CDM9 CD servo mechanism

mechanism is given in Figure 1.

A diode generates a laser beam that passes through a series of optical lenses in the OPU to give a spot on the disc surface. The light reflected from

the disc is measured on an array of photo diodes, mounted in the bottom of the OPU, yielding the signals required for position error information of the laser spot on the Compact Disc. The light intensity of the reflected beam is directly related to the percentage of the spot area that covers a pit. A schematic depiction of a track on an audio disc is shown in Figure 2.

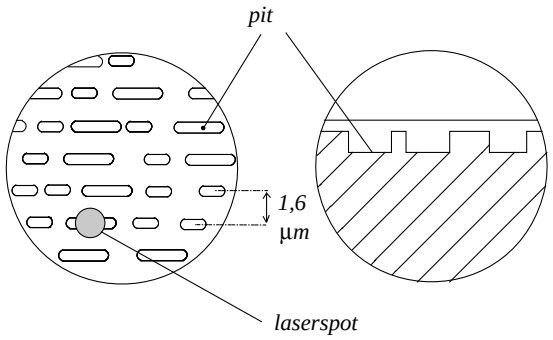

Fig. 2. Audio disc surface

Intensity of the reflected light is measured by a photo diode which converts light intensity into an electrical current. The audio signal is obtained through sampling at 44.1 kHz and adjusting the sampled signals for missing bits.

Following the track on the Compact Disc involves basically two control loops. First a radial control loop using a permanent magnet/coil system mounted on the radial arm, in order to position the laser spot in the radial direction orthogonal to the track. Secondly a focus control loop using an objective lens suspended by two parallel leaf springs and a permanent magnet/coil system, with the coil mounted in the top of the OPU to focus the laser spot on the disc. In Figure 3 a block diagram of the two control loops is shown. In here $G_a(q)$ denotes the transfer function of radial and focus actuator, K_{opu} the OPU, $K(q)$ the controller and $G_o(q) = -K_{opu}G_a(q)$. The variable q is the forward shift operator, yielding $x(t+1) = qx(t)$.

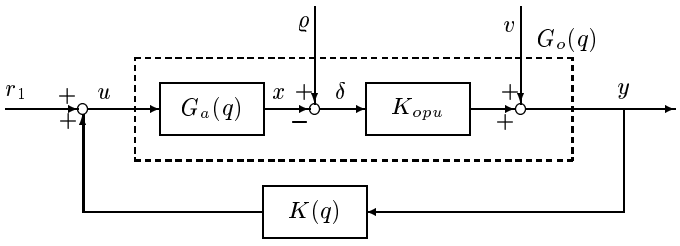

Fig. 3. Block diagram of the Compact Disc mechanism

The spot position error $\delta(t)$, which is the difference between the track position $\varrho(t)$ and the actuator position $x(t)$ in radial and focus direction, generates a (disturbed) error signal $y(t)$ via K_{opu}. This error signal $y(t)$ is led into the controller $K(q)$ and feeds the system $G_a(q)$ with the input $u(t)$. The signal $v(t)$ reflects the disturbance on the error signal $y(t)$. The absolute track position $\varrho(t)$ and actuator position $x(t)$ cannot be measured directly. Only the error signal $y(t)$ and the input $u(t)$ are available. For identification purposes an additional and known excitation signal $r_1(t)$, uncorrelated with the additive noise $v(t)$ will be injected into the control loops, as illustrated in Figure 3. In Figure 4 the amplitude frequency response of the system G_o is sketched.

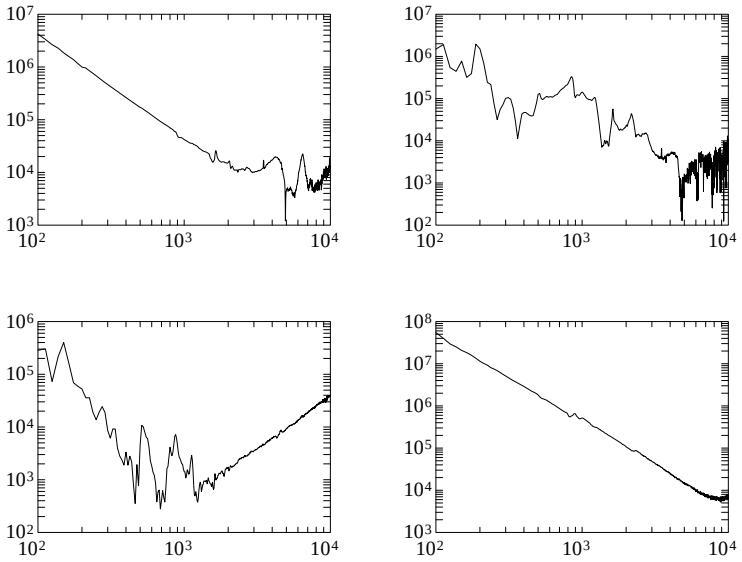

Fig. 4. Amplitude of spectral estimate of G_o; left upper figure is radial transfer, right lower figure is focus transfer; frequency axis is in Hz.

The radial actuator uses a conventional voice-coil motor to follow the spiral track recorded on the track of the reflective disc. As a result, the dominant dynamical behavior between voice-coil current and radial laser spot position can be described by a relatively simple 4th-order model that consists of a double integrator and the lateral bending mode of the radial arm [4]. This model adequately describes the dynamics of the radial actuator to design a conventional PID controller for track following. Traditionally, this PID controller is designed to achieve a closed-loop bandwidth of the Compact Disc radial servo loop of approximately 450 Hz, being a compromise between several conflicting factors [9].

Both control loops make the CD mechanism a 2-input 2-output system [4,2]. However for the illustration purposes of this chapter only the identification and control of the radial servo mechanism is considered here.

3 Control Relevant Modeling of Radial Actuator

The performance of the CD mechanism is determined mostly by the radial track following properties of the CD player. An increase of the radial closed-loop bandwidth can achieve increased shock disturbance rejection for better track following performance. For example, by trying to double the closed-loop bandwidth, track following errors can be reduced by an order of a magnitude. In case of the CDM9 mechanism discussed in this chapter, a redesign of the traditional PID controller is needed to nearly double the radial closed-loop bandwidth to 800 Hz.

Unfortunately, the relatively simple 4th-order model that consists of a double integrator and the lateral bending mode of the radial arm does not provide accurate enough information to redesign the PID controller at a higher radial closed-loop bandwidth. A straightforward redesign of the PID controller for a higher closed-loop bandwidth leads to ringing or even instability of the radial servo loop. This is illustrated in Figure 5 where excessive peaking in the measurement of the frequency response of the closed-loop sensitivity function can be observed.

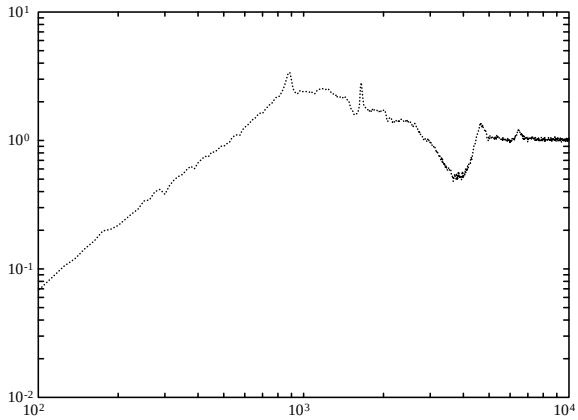

Fig. 5. Bode magnitude plot of measured sensitivity function $(1 + KG_o)^{-1}$ of the radial transfer for a PID controller design aiming at a radial closed-loop bandwidth of 800 Hz

In order to design an improved controller for the radial servo loop, a more accurate model of the radial actuator is needed. Additionally, for manageable control design the model should be kept low in complexity and should capture only those features in the radial actuator that are essential for the control design. Specifically, the radial actuator dynamics that cause the excessive peaking of the sensitivity function in Figure 5, needs to be accurately modelled. This can be achieved by a control-relevant approximate identification.

However since the to-be-designed controller is still unknown in the modelling stage, it has been advocated to use an iterative scheme of identification and control design, using the controller of step $i-1$, denoted with K to estimate a model $\hat{G}$ for step i and to design an improved controller $K_{\hat{G}}$ based on this model $\hat{G}$. In this chapter one step in such an iterative scheme will be illustrated involving an identification of a model $\hat{G}$ of the radial actuator G_o using an experimental situation where a known controller K is used. On the basis of the control relevant estimated model $\hat{G}$, we consider a redesign of the controller K and show the significance of the modeling procedure for the control design. Estimated model uncertainty bounds will be used to verify robust stability properties of the designed controller prior to its implementation.

4 Preliminaries and Notations

The closed-loop system of the radial servo loop in a Compact Disc player is written into the general feedback system $T(G_o, K)$[1] given in Figure 6, which will be used throughout this chapter.

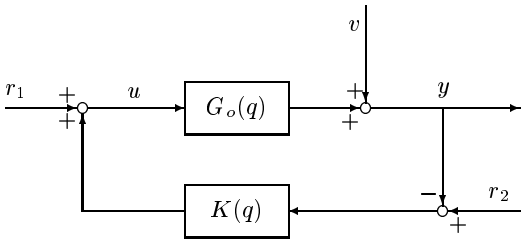

Fig. 6. General feedback system $T(G_o, K)$

In Figure 6, the signal $v(t)$ reflects the additive noise on the output $y(t)$ of the plant $G_o(q)$, which is assumed to be uncorrelated with the externally applied references signals $r_1(t)$ and $r_2(t)$. From an identification point of view, the signals $u(t)$ and $y(t)$ are measured, $v(t)$ is unknown and $r_1(t)$ and $r_2(t)$ are possibly at our disposal for experiment design purposes.

[1] for notational convenience the time shift operator q will generally be omitted.

Using Figure 6, the data from the closed-loop system $T(G_o, K)$ is described with the following equations.

$$\begin{bmatrix} y \\ u \end{bmatrix} = T(G_o, K) \begin{bmatrix} r_2 \\ r_1 \end{bmatrix} + \begin{bmatrix} I \\ -K \end{bmatrix} [I + G_o K]^{-1} v \tag{1}$$

where $T(G_o, K)$ reflects the general feedback matrix

$$T(G_o, K) = \begin{bmatrix} G_o \\ I \end{bmatrix} [I + K G_o]^{-1} \begin{bmatrix} K & I \end{bmatrix}. \tag{2}$$

This 2×2 transfer function reflects all feedback-relevant properties of the closed-loop system, such as sensitivity function (right lower part) and complementary sensitivity (left upper part).

A (possibly unstable) plant G can be described as a ratio of two stable transfer functions. In the theory of fractional representations [12] a pair of stable transfer functions (N, D) is called a *coprime factorization (cf)* of G if $G = ND^{-1}$ and N and D do not have unstable zeros that cancel in ND^{-1}. Additionally a coprime factorization (N_n, D_n) is called *normalized (ncf)* if it satisfies

$$N_n^* N_n + D_n^* D_n = I$$

where * denotes complex conjugate transpose.
A straightforward example of a (coprime) factorization of a plant G is

$$G = \frac{G(1 + KG)^{-1}}{(1 + KG)^{-1}}$$

showing that a possibly unstable plant G can be represented by fraction of two transfer functions that each are stable provided that K is a stabilizing controller.
Normalized coprime factorizations have the particular property that

$$|N_n(e^{i\omega})| \leq 1, \quad |D_n(e^{i\omega})| \leq 1.$$

Additionally it can be shown that for a normalized coprime factorization $G = N_n D_n^{-1}$ the McMillan degree of G is equal to the McMillan degree of N_n and D_n, in other words: the quotient operation of the two transfers does not lead to an increasing system order.
Coprime factorizations are unique up to multiplication with a stable and stably invertible transfer function. Normalized coprime factorizations are unique up to multiplication with a unitary matrix.

In the following lemma, the set of all coprime factorizations of a plant is described:

Lemma 1. *Let the plant G_o be controlled by a stabilizing controller K. Then all coprime factorizations (N, D) of G_o can be written as*

$$N = G_o[I + KG_o]^{-1}[I + KG_x]D_x$$
$$D = [I + KG_o]^{-1}[I + KG_x]D_x$$

with G_x any auxiliary system that is stabilized by K, having coprime factorization (N_x, D_x).

Proof. See [11].

5 Common Objectives in Identification and Control

The general feedback transfer function matrix $T(G,K)$ has been recognized as an important feedback property of the closed-loop system. It induces a feedback relevant topology, meaning that if two such operators are alike, the corresponding feedback controlled systems will have similar performances. Moreover, control design methods can be formulated on the basis of the minimization of the ∞-norm or 2-norm of the (frequency weighted) $T(G,K)$ matrix, [8,13].

The feedback transfer function matrix $T(G,K)$ encompasses both the information of the dynamics of the plant G and the controller K used to create the feedback connection. Therefore, for a given controller K, the (weighted) difference between $T(G_o,K)$ and $T(\hat{G},K)$ forms a so-called feedback relevant mismatch, caused by the difference between nominal model $\hat{G}$ and plant G_o.

This can be understood by considering a triangle inequality applied to $\|T(G_o,K)\|$ with $\|\cdot\|$ any norm or distance function, yielding ([10]):

$$\Big|\|T(\hat{G},K)\| - \|T(G_o,K) - T(\hat{G},K)\|\Big| \leq \|T(G_o,K)\| \tag{3}$$

$$\|T(G_o,K)\| \leq \|T(\hat{G},K)\| + \|T(G_o,K) - T(\hat{G},K)\|. \tag{4}$$

From (3) and (4) we see that by imposing the requirement

$$\|T(G_o,K) - T(\hat{G},K)\| \ll \|T(\hat{G},K)\| \tag{5}$$

similar performances for the controlled plant G_o and the controlled model $\hat{G}$ can be guaranteed. Therefore, constructing a model by minimizing the difference $\|T(G_o,K) - T(\hat{G},K)\|$ can be seen as a feedback relevant identification of the plant G_o.

The difference $\|T(G_o,C) - T(\hat{G},K)\|$ can be expressed in terms of the coprime factors of the plant G_o and the model $\hat{G}$. A direct identification of stable coprime factors then enables a unified approach to estimate stable and unstable models of plants operating under feedback controlled conditions. The results are summarized in the following section.

6 Estimation of Coprime Factorizations

6.1 Motivation

The framework for identification used in this chapter is based on the algebraic theory of fractional representations by directly estimating a coprime

factorization of the plant G_o using standard prediction error techniques. The motivation for using fractional representations from an *identification point of view* can be summarized as follows.

- The framework unifies the problem of dealing with unstable plants G_o and controllers K.
- The closed-loop identification problem can be recasted into an equivalent open loop identification of coprime plant factors. Consequently, the results in approximate open loop identification, based on prediction error methods like in [6], can be exploited.
- The fractional representation allows the formulation of an identification criterion that asymptotically matches a control-relevant plant-model mismatch $\|T(G_o, K) - T(\hat{G}, K)\|$, as described in the previous section.

Clearly, the first item is evident since coprime factorizations are defined to be stable. The last two items will be illustrated in subsequent sections.

6.2 Equivalent open loop identification

By using the equation of the data generating system given in (1) and the notation $r := r_1$ (assuming without loss of generality that $r_2 = 0$) we have

$$r = u + Ky. \tag{6}$$

Using this signal r, (1) can be simplified to

$$\begin{bmatrix} y \\ u \end{bmatrix} = \begin{bmatrix} G_o(I + KG_o)^{-1} \\ (I + KG_o)^{-1} \end{bmatrix} r + \begin{bmatrix} (I + KG_o)^{-1} \\ -K(I + KG_o)^{-1} \end{bmatrix} v.$$

If the controller K stabilizes the plant G_o, all elements of the matrix $T(G_o, K)$ will be stable. Hence both $G_o(I + KG_o)^{-1}$ and $(I + KG_o)^{-1}$ will be stable and can considered to be a coprime factorization (N_o, D_o) of the plant G_o. Moreover, the signal r defined in (6) is uncorrelated with the noise v of the closed-loop system given in Figure 6. This gives rise to an equivalent open loop identification problem by estimating a stable coprime factorization of the plant using r as input and $[y\ u]^T$ as output.

However, a coprime factorization is not unique and one can incorporate this freedom similarly as in [11], by introducing an additional filtering of the signal r, with $x := Fr$. Again using (1) and considering x as input signal in the identification, this yields a cf $(N_{o,F}, D_{o,F})$ of the plant G_o, with

$$\begin{cases} N_{o,F} = G_o(I + KG_o)^{-1}F^{-1} \\ D_{o,F} = (I + KG_o)^{-1}F^{-1} \end{cases} \tag{7}$$

where the filter F denotes the additional freedom in the cf of the plant G_o. According to the result of Lemma 1 the freedom in F can be characterized by

$$F = D_x^{-1}[I + KG_x]^{-1} = [D_x + KN_x]^{-1} \tag{8}$$

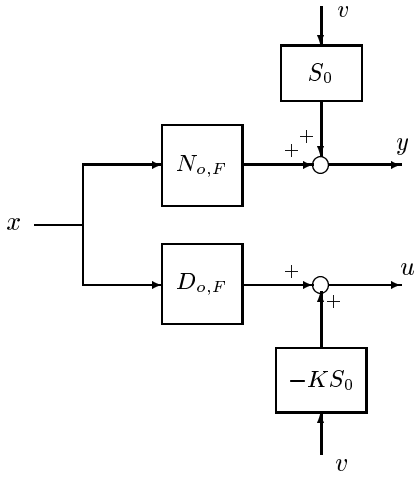

Fig. 7. Identification of coprime factors from closed-loop data

with $G_x = N_x D_x^{-1}$ any auxiliary model that is stabilized by K. The identification setup is depicted in Figure 7, where $S_o = (1 + KG_o)^{-1}$.

Since $x = Fr$ is uncorrelated with the noise v, the identification of the plant G_o from closed-loop measurements u and y is equivalent to an open loop identification of $N_{o,F}$ and $D_{o,F}$, considering x as input signal and $(y, u)^T$ as output. Constructing a (filtered) one-step-ahead prediction error for an Output Error (OE) type of model structure ([6]), we obtain:

$$\varepsilon(t,\theta) = \begin{bmatrix} y(t) \\ u(t) \end{bmatrix} - \begin{bmatrix} N(q,\theta) \\ D(q,\theta) \end{bmatrix} x(t) \tag{9}$$

$$\varepsilon_f(t,\theta) = L(q) I_{2\times 2} \varepsilon(t,\theta) \tag{10}$$

where $L(q)$ is an additional user-defined filtering of the prediction error. By applying a least squares identification criterion

$$\hat{\theta}_N = \arg\min_\theta \frac{1}{N} \sum_{t=0}^{N-1} \left\{ \varepsilon_f^T(t,\theta) \varepsilon_f(t,\theta) \right\} \tag{11}$$

it can be shown that for $N \to \infty$ and under the usual regularity conditions applied in prediction error identification, $\hat{\theta}_N \to \theta^\star$ with probability 1, with $\theta^\star = \arg\min_\theta \bar{V}(\theta)$ and

$$\bar{V}(\theta) = \frac{1}{2\pi} \int_{-\pi}^{\pi} \begin{bmatrix} N_{o,F}(e^{i\omega}) - N(e^{i\omega},\theta) \\ D_{o,F}(e^{i\omega}) - D(e^{i\omega},\theta) \end{bmatrix}^* \cdot \tag{12}$$

$$\begin{bmatrix} N_{o,F}(e^{i\omega}) - N(e^{i\omega},\theta) \\ D_{o,F}(e^{i\omega}) - D(e^{i\omega},\theta) \end{bmatrix} |L(e^{i\omega})|^2 \Phi_x(\omega)\, \mathrm{d}\omega. \tag{13}$$

In this expression $\Phi_x(\omega)$ is the auto spectral density of the signal $x(t)$. The interpretation of the frequency domain representation will be scrutinized in the following subsection.

6.3 Feedback relevant identification

The difference $\Delta T(G_o, \hat{G}, K) := T(G_o, K) - T(\hat{G}, K)$ introduced in Section 5 can be seen as a feedback relevant mismatch between the plant G_o and the nominal model $\hat{G}$. This mismatch can be expressed in terms of coprime factors. In [11] it has been analyzed that under the condition that $N_{o,F}$ and $D_{o,F}$ are normalized coprime factors, $\Delta T(G_o, \hat{G}, K)$ can be written as

$$\Delta T(G_o, \hat{G}, K) = \begin{bmatrix} N_{o,F} - \hat{N} \\ D_{o,F} - \hat{D} \end{bmatrix} F[K \quad I]. \tag{14}$$

Apparently the feedback relevant mismatch between G_o and $\hat{G}$ is a linear function of the difference between the cf of the model $\hat{G}$ and the corresponding cf of the plant G_o. By replacing the norm operator $\|\cdot\|$ by the H_2–norm [7] the following quadratic feedback relevant performance criterion $J_f(\theta)$, based on (14), can be defined

$$J_f(\theta) := \frac{1}{2\pi} \int_{-\pi}^{\pi} \begin{bmatrix} N_{o,F}(e^{i\omega}) - N(e^{i\omega}, \theta) \\ D_{o,F}(e^{i\omega}) - D(e^{i\omega}, \theta) \end{bmatrix}^* \cdot \begin{bmatrix} N_{o,F}(e^{i\omega}) - N(e^{i\omega}, \theta) \\ D_{o,F}(e^{i\omega}) - D(e^{i\omega}, \theta) \end{bmatrix} |F|^2 (1 + |K|^2) \, \mathrm{d}\omega. \tag{15}$$

Comparing the feedback relevant performance criterion $J_f(\theta)$ in (15) with the frequency domain representation of the least squares OE-minimization given in (13), it follows that the two criteria are equivalent in case

$$|L(e^{i\omega})|^2 \Phi_x(\omega) = |F(e^{i\omega})|^2 \cdot (1 + |K(e^{i\omega})|^2)$$

or equivalently

$$|L(e^{i\omega})|^2 = c_1 \frac{1 + |K(e^{i\omega})|^2}{\Phi_r(\omega)}$$

where $c_1 \neq 0$ is an arbitrary constant and $\Phi_r(\omega)$ is the auto spectral density of the excitation signal r.

As mentioned above, for the validity of (14) the accessed plant factors $N_{o,F}$, $D_{o,F}$ have to be normalized. This can be (approximately) achieved by using a normalized cf (N_x, D_x) of an auxiliary model G_x that approximately equals G_o. From (7) and (8) it then follows that $N_{o,F}$, $D_{o,F}$ become normalized too; a more detailed explanation can be found in [11].

7 Application to CD Radial Actuator

7.1 Data acquisition

Measurements of the Compact Disc radial servo loop have been obtained from an experimental set up of a Compact Disc player provided by Philips Research Laboratories in Eindhoven, the Netherlands. This experimental set up is used to gather a closed-loop measured time sequence of 8192 data points of the voltage input signal $u(t)$ to the radial actuator and the track position error signal $y(t)$.

For the closed-loop experiments, the same (and known) PID controller is used that caused the excessive peaking in the sensitivity function indicated in Figure 5. During the closed-loop experiment, a periodic reference signal $r(t) = r_1(t)$ is added to the input signal u constructed by taking one realization of 1024 data points from a white noise stochastic process, and concatenating this signal 8 times. The gathered time sequence of $u(t)$ and $y(t)$ and the knowledge of the controller K are used to perform a control relevant estimation of a coprime factorization of the radial actuator G_o.

7.2 Estimation of coprime factors

To access a coprime factorization of G_o from a closed-loop experiment, first a filter F and the signal x must be created. Using a relatively simple model that consists of a double integrator and the lateral bending mode of the radial arm, a 4th-order auxiliary model G_x with a normalized cf (N_x, D_x) is created. The coprime factor model (N_x, D_x) is used to create the filter F and the signal x, according to $x = Fr$ with F given by (8).

Subsequently, a relatively high order (order 32) model of the coprime factors of the radial actuator is estimated. This relatively high-order coprime factor model is used to update the knowledge of the coprime factorization (N_x, D_x) of the auxiliary model G_x. An amplitude Bode plot of the updated high-order coprime factor model (N_x, D_x) is given in Figure 8(left). The amplitude Bode plot of the model (N_x, D_x) is compared with a measured frequency response using the signals x and (y, u).

It should be noted that the relatively high order (32) coprime factor model (N_x, D_x) depicted in Figure 8 is not the actual low-order control relevant model of the radial actuator that needs to be estimated. The high-order factorization (N_x, D_x) is used *only* to create the filter $F = (D_x + KN_x)^{-1}$ and therefore the order is not of crucial importance. With the updated information of the auxiliary model G_x in the form of the high-order coprime factor model (N_x, D_x), a new filter F and signal x can be constructed for identification purposes. With the updated and more accurate auxiliary model, the filter F will simplify the dynamics of the coprime factors of the plant in (7) and facilitate the minimization of the control relevant criterion given in (14). In the right picture of Figure 8 it is indicated that with the chosen filter

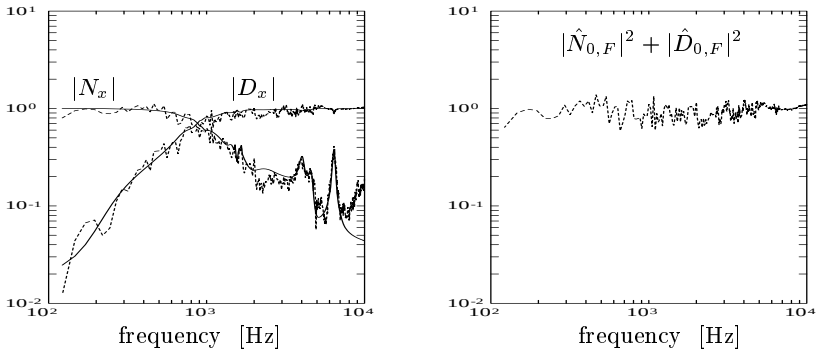

Fig. 8. Left: Bode magnitude plots of coprime factors (N_x, D_x) of auxiliary model G_x; spectral estimate (dashed) and 32nd-order parametric estimate (solid). Right: $|N_{0,F}|^2 + |D_{0,F}|^2$ induced by the prefilter $F = (D_x + KN_x)^{-1}$.

F, the accessible coprime plant factors $(N_{o,F}, D_{o,F})$ are (almost) normalized. The verification of $|N_{o,F}|^2 + |D_{o,F}|^2 = 1$ is being done on the basis of spectral estimates.

For approximation and control applications, a low-order and control relevant coprime factor model $(\hat{N}, \hat{D})$ needs to be estimated. A Bode plot of a relative low (10th) order coprime factor model $(\hat{N}, \hat{D})$ is given in Figure 9. In these plots the model $(\hat{N}, \hat{D})$ is compared with a measured frequency response using the signals x and (y, u).

Compared with the spectral estimate of the coprime factorization of the radial actuator, it can be observed from Figure 9 that the essential dynamics which would explain the excessive peaking of the sensitivity function in Figure 5 has been captured well in the 10th-order coprime factor model.

8 Control Design and Stability Robustness

The improved knowledge of the radial actuator in the form of the model $\hat{G} = \hat{N}/\hat{D}$ can be used to redesign the controller K. This controller synthesis is carried out by means of the weighed optimization:

$$K_{\hat{G},\nu_b} = \arg_{\bar{K}} \min \left\| \begin{bmatrix} W_{\nu_b}\hat{G} \\ 1 \end{bmatrix} [1 + \tilde{K}\hat{G}]^{-1} [\tilde{K}/W_{\nu_b} \quad 1] \right\|_\infty \tag{16}$$

where W_{ν_b} is a filter, designed for a nominal design bandwidth of ν_b Hz. The controller synthesis is an H_∞ loop shape design according to McFarlane and Glover [8,1], which is known to optimizes robustness against additive perturbations of the coprime factors of the model. The weighting filter W_{ν_b} is designed to shape the loop transfer $W_{\nu_b}\hat{G}$ to achieve a prespecified bandwidth, and additional robustness properties are achieved by solving the optimization

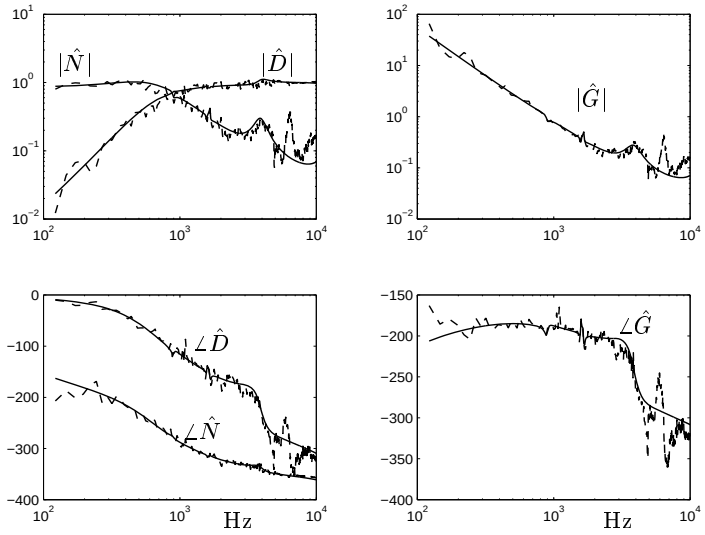

Fig. 9. Amplitude (upper) and phase (lower) Bode plots of spectral estimate (dashed) and parametric estimate (solid) of low (10th) order coprime factors $(\hat{N}, \hat{D})$ (left) and model $\hat{G} = \hat{N}/\hat{D}$ (right)

problem (16). The weighting function applied here is constructed according to:

$$W_{\nu_b} := \frac{K}{s} \cdot \frac{\tau_1 s + 1}{\tau_2 s + 1}$$

with K, τ_1, τ_2 appropriately chosen to achieve a nominal design bandwidth of ν_b. W_{ν_b} incorporates a phase lead in the cross-over frequency region which allows the stabilization of a double integrator; it incorporates an integrator to guarantee good disturbance attenuation for low frequencies; additionally there is a controller roll-off for high frequencies. This control design procedure was used to design a new (improved) feedback controller $K_{\hat{G}}$ of order 8 with a nominal design bandwidth of $\nu_b = 800Hz$. An amplitude Bode plot is depicted in Figure 10.

Before the newly designed controller can be safely implemented, it has to be verified whether it will stabilize the radial control loop. One of the implemented procedures is directed towards estimating an upper bound on the additive error of the normalized coprime factors $(\hat{N}, \hat{D})$ being estimated. Denoting:

$$N_{o,F}(e^{i\omega}) = \hat{N}(e^{i\omega}) + \Delta_N(e^{i\omega}) \tag{17}$$

$$D_{o,F}(e^{i\omega}) = \hat{D}(e^{i\omega}) + \Delta_D(e^{i\omega}) \tag{18}$$

the uncertainty bounding procedure of [3] is a mixed deterministic/probabilistic approach which is fully compatible with the prediction error identification

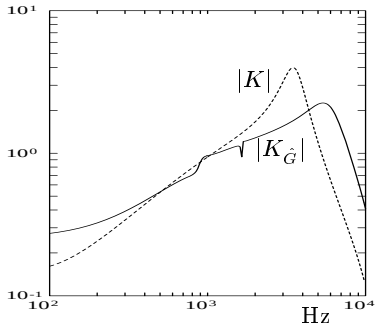

Fig. 10. Amplitude plots of traditional PID controller K (dashed) and newly redesigned 8th-order radial servo controller $K_{\hat{G}}$ (solid)

framework, delivering upper bounds on the additive model errors $|\Delta_N(e^{i\omega})|$ and $|\Delta_D(e^{i\omega})|$. It provides frequency dependent upper bounds with an a priori chosen probability level per frequency:

$$\left.\begin{array}{l} |\Delta_D(e^{i\omega})| \leq \gamma_1(\omega) \\ |\Delta_N(e^{i\omega})| \leq \gamma_2(\omega) \end{array}\right\} \text{ w.p. } \geq \alpha \tag{19}$$

where α is a prespecified probability. The uncertainty bounding procedure combines a deterministic (worst-case) bound on the undermodelling (bias) error, with a stochastic confidence interval for noise-induced uncertainty. The bounding procedure is performed on the basis of periodic excitation signals. Results of this procedure applied to the estimated coprime factors are depicted in Figure 11, showing three upper bounds on the additive errors, related to three different choices of α.

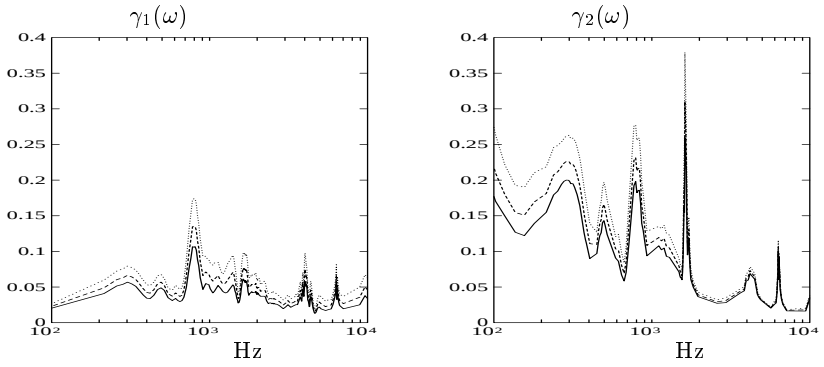

Fig. 11. Upper bounds $\gamma_1(\omega)$ and $\gamma_2(\omega)$ on additive model error of normalized coprime factors $|\hat{D}(e^{i\omega})|$ (left) and $|\hat{N}(e^{i\omega})|$ (right) for $\alpha = 90\%$ (—), 99% (- -) and 99.9% ($\cdots$)

Using this knowledge of an upper bound on (Δ_N, Δ_D) we can check stability robustness properties of the closed-loop system by employing the following result. Provided that $\hat{G} = \hat{N}\hat{D}^{-1}$ is stabilized by $K = D_k^{-1}N_k$, the set of plants $G = ND^{-1}$ determined by

$$N(e^{i\omega}) = \hat{N}(e^{i\omega}) + \Delta_N(e^{i\omega}), \qquad |\Delta_N(e^{i\omega})| \leq \gamma_1(\omega) \tag{20}$$

$$D(e^{i\omega}) = \hat{D}(e^{i\omega}) + \Delta_D(e^{i\omega}), \qquad |\Delta_D(e^{i\omega})| \leq \gamma_2(\omega) \tag{21}$$

is stabilized by K if ([1]): $\|[N_k \ D_k] \begin{bmatrix} \Delta_N \\ \Delta_D \end{bmatrix} \hat{\Lambda}^{-1}\|_\infty < 1$,

with $\hat{\Lambda} = \tilde{D}_k\hat{D} + \tilde{N}_k\hat{N}$.

This condition can be checked by verifying whether

$$\frac{1}{|\hat{\Lambda}(e^{i\omega})|}[|N_k(e^{i\omega})|\gamma_1(\omega) + |D_k(e^{i\omega})|\gamma_2(\omega)] < 1 \quad \text{for all } \omega. \tag{22}$$

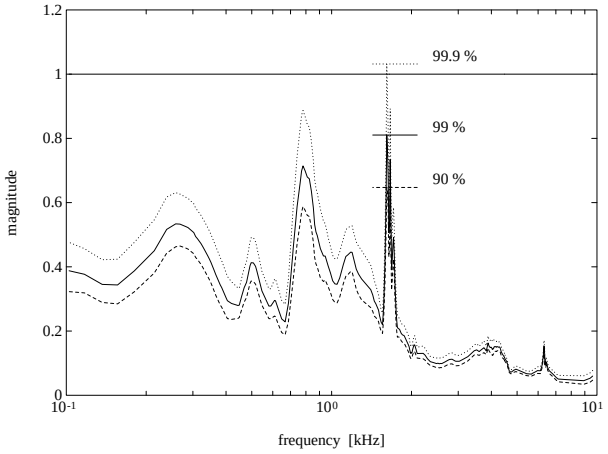

Fig. 12. Stability robustness tests of the new controller for point wise confidence intervals on the estimated coprime factors at three probability levels

This sufficient condition for robust stability has been implemented and its result is depicted in Figure 12. It shows that even for an α-level of larger than 99% robust stability can be guaranteed. If α is chosen 99.9% the sufficient condition is not satisfied. However, this result is assessed to be sufficiently promising to allow implementing the controller. Successful implementation of the controller $K_{\hat{G}}$ using a DSP environment yields a high-performance closed-loop system with a bandwidth of approximately 800 Hz without excessive peaking of the sensitivity function, leading to improved disturbance rejection. This has been illustrated in Figure 13.

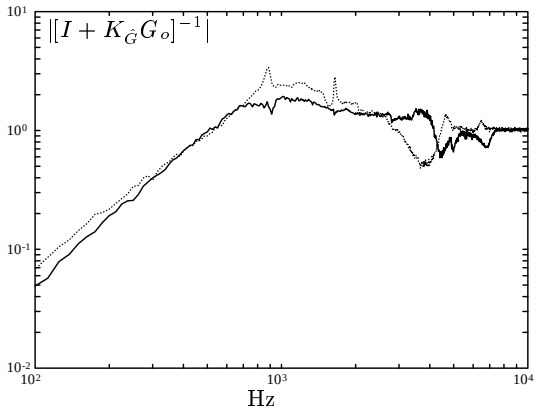

Fig. 13. Amplitude Bode plots of sensitivity function with traditional PID controller (dashed) and newly redesigned 8th-order radial servo controller $K_{\hat{G}}$ (solid)

9 Summary

In this chapter a control relevant parametric identification scheme is applied to a Compact Disc radial servo system, using the well known prediction error methods. In the identification methodology, the problem of approximate (low-order) identification and closed-loop experiments are addressed. The problems arising from the closed-loop and approximate identification have been handled using an identification based on fractional representations. By appropriate filtering this yields a manageable control-relevant identification of the plant, while pertaining to low-order models. Additionally, uncertainty bounding techniques have been shown to allow for a practically applicable stability robustness test that is performed prior to controller implementation. The designed and implemented controller has been shown to lead to the desired improved performance. A similar identification approach extended to the multivariable case, and in combination with a *robust* control design procedure, is incorporated in Chapter **??** of this book.

10 Acknowledgements

The authors acknowledge the contributions of Peter Bongers, Douwe de Vries, Hans Dötsch, Okko Bosgra and Maarten Steinbuch to the results presented here, and the support of Philips Research in providing the Compact Disc hardware.

References

1. P.M.M. Bongers and O.H. Bosgra. Low order robust H_∞ controller synthesis. In *Proc. 29th IEEE Conf. Decis. Control*, pages 194–199, Honolulu, HI, 1990.
2. R.A. de Callafon, P.M.J. Van den Hof, and M. Steinbuch. Control relevant identification of a compact disc pick-up mechanism. In *Proc. 32nd IEEE Conf. Decis. Control*, pages 2050–2055, San Antonio, TX, USA, 1993.
3. D.K. de Vries and P.M.J. Van den Hof. Quantification of uncertainty in transfer function estimation: a mixed probabilistic - worst-case approac. *Automatica*, 31:543–557, 1995.
4. W. Draijer, M. Steinbuch, and O.H. Bosgra. Adaptive control of the radial servo system of a compact disc player. *Automatica*, 28:455–462, 1992.
5. M.R. Gevers. Towards a joint design of identification and control? In *Essays on Control: Perspectives in the Theory and its Applications*, pages 111–151, Birkhäuser, Boston, 1993. H.L. Trentelman and J.C. Willems (Eds.).
6. L. Ljung. *System Identification: Theory for the User*. Prentice-Hall, Englewood Cliffs, NJ, USA, 1987.
7. J.M. Maciejowski. *Multivariable Feedback Design*. Addison-Wesley, Wokingham, England, 1989.
8. D. McFarlane and K. Glover. A loop shaping design procedure using H_∞ synthesis. *IEEE Trans. Autom. Control*, 37:759–769, 1992.
9. M. Steinbuch, G. Schootstra, and O.H. Bosgra. Robust control of a compact disc player. In *Proc. 31st Conf. Decis. and Control*, pages 2596–2600, Tucson, AZ, USA, 1992.
10. P.M.J. Van den Hof and R.J.P. Schrama. Identification and control - closed loop issues. *Automatica*, 31:1751–1770, 1995.
11. P.M.J. Van den Hof, R.J.P. Schrama, R.A. de Callafon, and O.H. Bosgra. Identification of normalised coprime plant factors from closed-loop experimental data. *European Journal of Control*, 1(1):62–74, 1995.
12. M. Vidyasagar. *Control System Synthesis: A Factorization Approach*. MIT Press, Cambridge, Massachusetts, USA, 1985.
13. K. Zhou, J.C. Doyle, and K. Glover. *Robust and Optimal Control*. Prentice-Hall, Upper Saddle River, New Jersey, USA, 1996.

Index